



Audio Engineering Society

Convention Paper 9054

Presented at the 136th Convention
2014 April 26–29 Berlin, Germany

This paper was peer-reviewed as a complete manuscript for presentation at this Convention. Additional papers may be obtained by sending request and remittance to Audio Engineering Society, 60 East 42nd Street, New York, New York 10165-2520, USA; also see www.aes.org. All rights reserved. Reproduction of this paper, or any portion thereof, is not permitted without direct permission from the Journal of the Audio Engineering Society.

Dynamic Measurement of Loudspeaker Suspension Parameters Using an Active Harmonic Control Technique

Antonin Novak^{1,2}, Pierrick Lotton¹ and Laurent Simon¹

¹Laboratoire d'Acoustique de l'Université du Maine, UMR CNRS 6613, Le Mans, France

²Orkidia Audio, Technopole Izarbel, 64210 Bidart, France

Correspondence should be addressed to Antonin Novak (antonin.novak@orkidia-audio.com)

ABSTRACT

A new nondestructive technique to measure the nonlinear suspension parameters (stiffness K_{ms} and mechanical resistance R_{ms}) of a loudspeaker using an active harmonic control technique is presented. The goal of the active harmonic control is to eliminate the higher harmonics from the displacement signal so that a purely harmonic motion of the diaphragm is ensured. The nonlinear stiffness K_{ms} is then measured as a function of instantaneous and peak displacement; the mechanical resistance R_{ms} is measured as a function of velocity. A frequency dependence of these parameters is also discussed.

1. INTRODUCTION

A traditional electrodynamic loudspeaker is equipped with a suspension which is usually formed by a surround attached to the outer edge of the diaphragm and a spider attached to the voice-coil. The purpose of the suspension is to center and adjust the voice-coil in the gap and to allow an axial motion of the diaphragm while preventing lateral motion or rocking. In an ideal case the suspension

behaves as a spring defined by its mechanical stiffness K_{ms} or by mechanical compliance C_{ms} (inverse value of the stiffness K_{ms}). In a less ideal case the suspension is lossy, being represented by mechanical resistance R_{ms} . The combination of the stiffnesses K_{ms} and the mechanical resistance R_{ms} along with the moving mass (cone + air load) M_{ms} will determine a simple resonant circuit which is usually used in loudspeaker modeling [1, 2].

Unfortunately, the traditional linear lumped parameter approach of a simple resonant circuit representing the suspension part is not sufficient in loudspeaker modeling. In a real world loudspeaker, the suspension shows hysteretic and nonlinear behavior. Due to both the geometry of the suspension and the material properties of the surround and the spider, and due to the physical phenomena such as adhesive friction, nonlinear viscoelastic effects and many others [3], the stiffness K_{ms} and the mechanical resistance R_{ms} cannot be considered as constant.

Many of these effects has been considered in loudspeaker modeling in the following works. An empirical model describing the effects of viscoelasticity in loudspeaker suspension has been presented by Knudsen in [4]. Thorborg et al. has presented in [5] a lumped parameter model for the dynamic loudspeaker which incorporates a mechanical resistance R_{ms} proportional to frequency taking into account the frequency dependence of the mechanical damping. In Thorborg's recent paper [6], the model is further refined to include frequency dependence of compliance C_{ms} . Klippel has developed a dynamic technique to measure the separated suspension parts pneumatically [7]. He has shown that the stiffness K_{ms} for a given frequency f depends not only on instantaneous displacement x but also on the peak displacement x_{peak} . He also suggests that the mechanical resistance R_{ms} should vary with instantaneous velocity and displacement.

In this paper we present a nondestructive dynamic technique to measure the stiffness K_{ms} as a function of instantaneous and peak displacement and the mechanical resistance $R_{ms}(v)$ as a function of instantaneous velocity of an electrodynamic loudspeaker. The whole loudspeaker is excited electrically and the velocity v and current i are measured. An active harmonic control is used to ensure a purely harmonic displacement and velocity of the diaphragm.

2. PURELY HARMONIC DIAPHRAGM MOTION

The method presented in this paper is a nondestructive method that necessitates a purely harmonic motion of the diaphragm. An active harmonic control, briefly described in this section, ensures having the displacement $x(t)$, the velocity $v(t)$ and the accel-

eration $a(t)$ of the diaphragm to be almost purely sinusoidal.

2.1. Harmonic excitation

In the ideal case the displacement of a loudspeaker diaphragm is supposed to follow accurately the applied signal. In reality, however, it is not true for two main reasons. First, from the linear point of view, applying a sine wave with angular frequency ω_0 as input voltage results in a sine displacement with the same angular frequency ω_0 phase shifted by φ_1 according to the transfer function. Second, from the nonlinear point of view, additional content is added at the harmonics of the fundamental frequency causing harmonic distortion. Applying a voltage $u(t)$ to the loudspeaker speaker

$$u(t) = U_1 \sin(\omega_0 t) \quad (1)$$

causes a displacement of the diaphragm

$$x(t) = X_1 \sin(\omega_0 t + \varphi_1) + e(t), \quad (2)$$

where

$$e(t) = \sum_{k=2}^{\infty} X_k \sin(k\omega_0 t + \varphi_k) \quad (3)$$

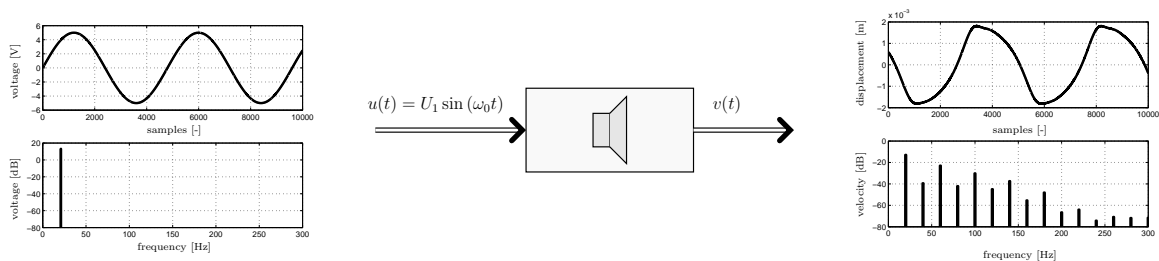
is the additional content caused by the nonlinear behavior of the loudspeaker.

2.2. Active Control Technique

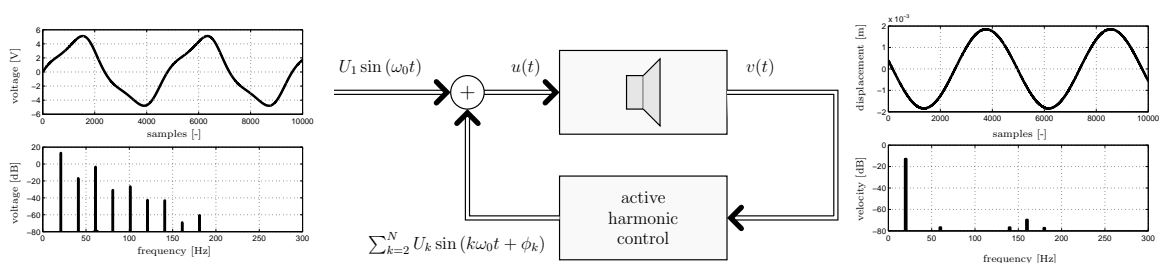
To ensure a purely harmonic motion of the diaphragm, an active harmonic control technique is used. This technique adds higher harmonics to the voltage to minimize the signal $e(t)$. The excitation voltage can be described by

$$u(t) = U_1 \sin(\omega_0 t) + \sum_{k=2}^N U_k \sin(k\omega_0 t + \phi_k), \quad (4)$$

N being the number of harmonics added to the input voltage. The goal of the active harmonic control is to eliminate the higher harmonics contained in the displacement signal so that only the fundamental response remains. It searches for the best combination of amplitudes U_k and phases ϕ_k , $k \in \langle 2, N \rangle$ that relates to producing the least error signal $e(t)$ and thus linearizing the displacement signal $x(t)$. Such a combination of amplitudes U_k and phases ϕ_k is the best solution for a given excitation frequency ω_0 and amplitude U_1 . Different frequency ω_0 or amplitude U_1



(a) No active control applied. Loudspeaker excited with a pure harmonic signal (time waveform and spectrum of the voltage signal are plotted on the left side), the diaphragm displacement being distorted as depicted on the right side (time waveform of the displacement above and magnitude spectrum of the velocity below).



(b) Active harmonic control applied. Excitation voltage signal is distorted (time waveform and spectrum of the voltage signal are plotted on the left side) in a such way that the diaphragm displacement is almost a pure harmonic signal as depicted on the right side (time waveform of the displacement above and magnitude spectrum of the velocity below).

Fig. 1: Simplified block scheme of the active harmonic control with an example of a particular case where a loudspeaker is excited at 20 Hz. Real signals captured during the measurement are depicted.

leads to a different set of amplitudes U_k and phases ϕ_k , $k \in \langle 2, N \rangle$ that relates to producing the least error signal $e(t)$.

An example of the active harmonic control is shown in Fig. 1. The loudspeaker is first excited with a harmonic voltage with frequency 20 Hz. The time waveform of diaphragm displacement and the magnitude spectra of the measured velocity is depicted in Fig. 1a. Next, applying the active harmonic control, higher harmonics are added to the voltage excitation to diminish the higher harmonics from the displacement and velocity signal Fig. 1b.

3. MEASUREMENT SETUP

In this paper a PIONEER B13ER89-51D boomer is chosen as a test object. Before measuring the mechanical properties of its suspension, two important parameters of the loudspeaker must be known: the force factor $Bl(x)$ as a function of displacement

x and the moving mass M_{ms} . Klippel loudspeaker analyzer has been used to estimate these parameters resulting in moving mass $M_{ms} = 10.7$ g and force factor $Bl(x)$ expressed as a polynomial with $Bl(0) = 5.93$ NA.¹

Once the force factor $Bl(x)$ and the moving mass M_{ms} of the loudspeaker under test are known, the measurement of the mechanical parameters can be set up according to Fig. 2. To measure the current, a Current Probe Fluke i50s with insertion impedance lower than 10 m Ω within the audible bandwidth is used. In addition, a single-point vibrometer Polytec (OFV-503, OFV-505) is used to make non contact measurement of the diaphragm vibrations. The loudspeaker is excited at a given frequency f_0 and amplitude U_1 and the active harmonic control described in the previous section is used. Once the

¹ $Bl(x) = \sum_{k=0}^6 p_k x^k$, where $p_6 = -2.0597e+14$, $p_5 = -3.5656e+11$, $p_4 = 6.2767e+09$, $p_3 = 1.6035e+07$, $p_2 = -1.8382e+05$, $p_1 = -396.22$, $p_0 = 5.9302$.

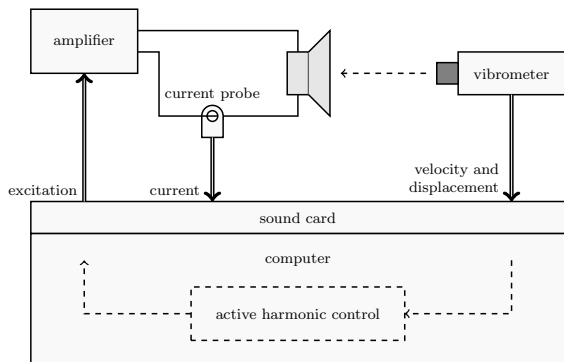


Fig. 2: The block scheme of experimental setup.

higher harmonics of the diaphragm velocity signal are diminished to the noise floor level, a few periods of the current $i(t)$ and velocity $v(t)$ are recorded. The process is repeated for different excitation levels U_1 and frequencies f_0 .

4. SUSPENSION ANALYSIS

In this section, the analysis procedure will be described for the case of an excitation at $f_0 = 40$ Hz with 10 different amplitude levels chosen to displace the diaphragm from small (0.2 mm) to large (1.5 mm) excursions. The highest excitation level is set to $U_1 = 2.5$ V. The difference between two successive levels is set to 2 dB giving 18 dB difference between the highest and the lowest excitation levels.

Assuming a purely harmonic displacement obtained using the active harmonic control described above,

$$x(t) = X_1 \sin(\omega_0 t + \varphi_1) \quad (5)$$

the velocity and the acceleration of the diaphragm are also described by a harmonic signal as

$$v(t) = V_1 \cos(\omega_0 t + \varphi_1) \quad (6)$$

$$a(t) = -A_1 \sin(\omega_0 t + \varphi_1), \quad (7)$$

where $V_1 = \omega_0 X_1$ and $A_1 = \omega_0^2 X_1$. This property is an important feature for estimation of the suspension parameters K_{ms} and R_{ms} . It helps us not only to provide a single frequency excitation, which can be useful to separate properly the frequency dependency of these parameters, but also to ensure that

displacement and acceleration are at their peak values when velocity is zero and vice versa.

4.1. Driving Force vs. Displacement

The diaphragm motion is described by its displacement $x(t)$ and the driving force $F(t) = Bl(x(t))i(t)$ which is related to the current $i(t)$. Any other forces, such as reluctance force proportional to the square of the current, or the drag force caused by eddy currents can, if known, be taken into account. The second law of motion can be then written

$$F(t) = M_{ms}a(t) + R_{ms}v(t) + K_{ms}x(t), \quad (8)$$

where $M_{ms}a(t)$ is the *inertial force*, $R_{ms}v(t)$ is the *damping force* and where $K_{ms}x(t)$ is the *restoring force*. In Fig. 3, the measured driving force $F(t)$ is plotted versus displacement $x(t)$ for several amplitudes of the excitation signal. The shape of

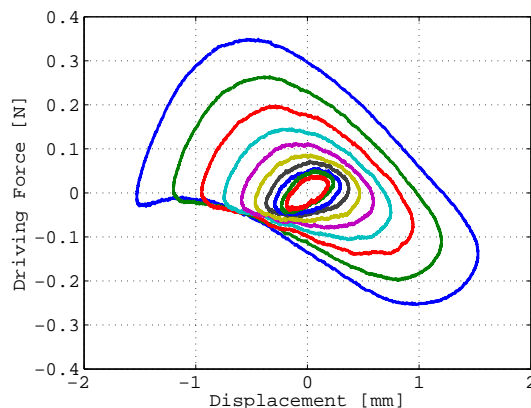


Fig. 3: Driving force $F(t)$ plotted versus displacement $x(t)$ for various excitation levels at 40 Hz.

the curves in the force-displacement plot is more and more deformed with increasing amplitude of the excitation signal due to the nonlinear behavior of the loudspeakers suspension. For small amplitudes, the force-displacement plot is an ellipse. The resulting curve for large amplitudes reveals a nonlinear response. Moreover, a symmetry breaking is obvious with increasing amplitude. At small amplitudes the curve has almost a symmetrical shape whilst at higher amplitudes it becomes more and more asymmetrical.

4.2. Restoring and Dumping Forces

Knowing the moving mass M_{ms} and the acceleration $a(t)$, we can put the inertial force $M_{ms}a(t)$ to the left side of Eq. (8) resulting in

$$F(t) - M_{ms}a(t) = R_{ms}v(t) + K_{ms}x(t). \quad (9)$$

The driving force $F(t)$ minus inertial force $M_{ms}a(t)$ is equivalent to the sum of restoring and damping force. In Fig. 4 the resulting (restoring + damping) force is plotted versus displacement and velocity respectively. The deformation of the curves still increases with amplitude of the excitation signal as well as the asymmetry. The force necessary to displace the diaphragm in negative direction to its peak value (-1.5 mm) exceeds -1 N, whilst in the positive direction (1.5 mm) the force does not reach 1 N.

4.3. Mechanical Resistance

To estimate the mechanical resistance R_{ms} we define the time moments t_{x_0} in which the diaphragm displacement is instantaneously zero $x(t_{x_0}) = 0$. Note, that according to Eq. (5-7) the velocity $v(t_{x_0}) = \pm V_1$ is equal to the positive or negative peak velocity depending on the direction of the motion, and the acceleration $a(t_{x_0})$ is also equal to zero. These zero displacement points are highlighted in Fig. 4 by circles.

Writing Eq. (9) for these time moments t_{x_0} yields to

$$F(t_{x_0}) - M_{ms}a(t_{x_0}) = R_{ms}v(t_{x_0}) + K_{ms}x(t_{x_0}) \quad (10)$$

that yields in

$$F(t_{x_0}) = R_{ms}v(t_{x_0}). \quad (11)$$

The mechanical resistance R_{ms} , valid for the t_{x_0} moments, is expressed as

$$R_{ms} = \frac{F(t_{x_0})}{v(t_{x_0})}. \quad (12)$$

In Fig. 5, the mechanical resistance R_{ms} is plotted versus peak velocity $\pm V_1$. It is obvious from the plot that the mechanical resistance R_{ms} is not constant but varies with the peak velocity $\pm V_1$. Moreover, the results for different amplitudes of the excitation signal (different peak velocities $\pm V_1$) forms a nice pattern that can be easily fitted using a polynomial curve fit (dashed curve in Fig. 5). This gives rise to

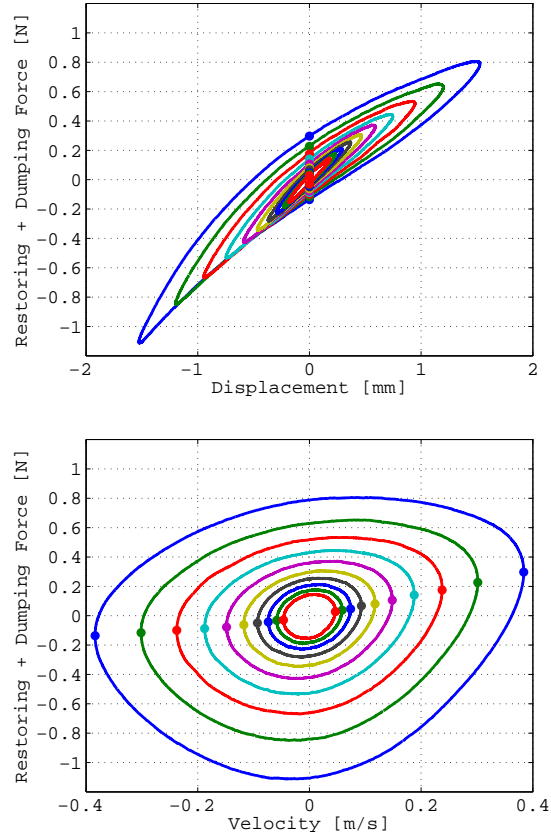


Fig. 4: $F(t) - M_{ms}a(t)$ (equivalent to the restoring plus damping force) plotted versus displacement $x(t)$ (above) and velocity $v(t)$ (below) for different amplitudes of the excitation signal at 40 Hz. Zero displacement points t_{x_0} are highlighted by circles.

the hypothesis that the mechanical resistance R_{ms} obtained as a function of peak velocity can be generalized as a function of instantaneous velocity for all excitation levels ($R_{ms}(\pm V_1) \equiv R_{ms}(v)$). It allows us to define the damping force as $R_{ms}(v)v(t)$. Putting it together with the inertial force $M_{ms}a(t)$ to the left side of Eq. (8) we get

$$F(t) - M_{ms}a(t) - R_{ms}(v)v(t) = K_{ms}x(t). \quad (13)$$

4.4. Mechanical Stiffness

As shown in Eq. (13), the driving force minus the inertial and the damping force results in the restor-

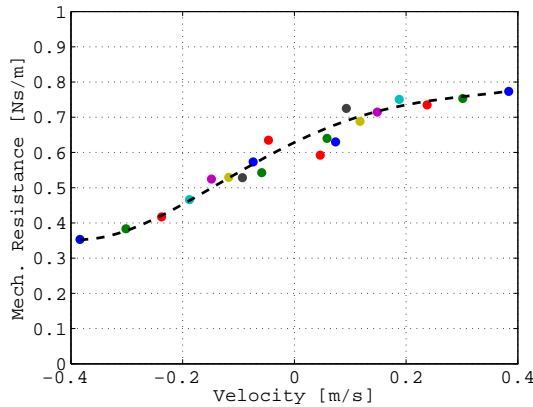


Fig. 5: Mechanical resistance R_{ms} versus peak velocity $\pm V_1$ for different amplitudes of the excitation signal at 40 Hz. Polynomial fit (order 5) is plotted dashed.

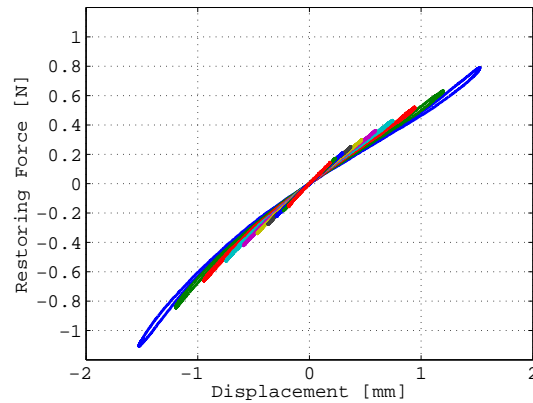


Fig. 6: Restoring force (equivalent to $F(t) - M_{ms}a(t) - R_{ms}(v)v(t)$) plotted versus displacement $x(t)$ for different amplitudes of the excitation signal at 40 Hz.

ing force. The curves in Fig. 6, where the restoring force is plotted versus displacement, has almost no inside-area. In other words, the path of curve is almost the same when tracing the curve upwards or downwards indicating no hysteretic relation between the restoring force and the displacement. However, Fig. 6 shows that the restoring force - displacement curve exhibits nonlinear behavior.

By definition the stiffness K_{ms} is the slope of restoring force - displacement curve at any given point. The slope at the origin ($x = 0$) is obviously steeper for lower amplitudes of the excitation signal than for the higher ones indicating a variation of the stiffness K_{ms} with the amplitude of the excitation signal. Using a polynomial fit of the force - displacement curve on Fig. 6 and estimating the shape of these fitted curves allows to estimate the mechanical stiffness K_{ms} for each displacement x . The resulting K_{ms} as a function of the instantaneous displacement and the amplitude of the excitation signal is shown in Fig. 7.

The variation with both, the instantaneous displacement and the amplitude of excitation signal is obvious. The stiffness decreases dramatically with the amplitude of the excitation level. For small signal levels yielding in a small peak displacement (0.2 mm) the estimated stiffness K_{ms} is 800 N/m. For large

signal levels yielding in a large peak displacement (1.5 mm) the stiffness K_{ms} varies between 470 and 720 N/m. Moreover, the curves show a small geometrical asymmetry indicating that the minimum of the stiffness curve is not equal to the rest position of the suspension.

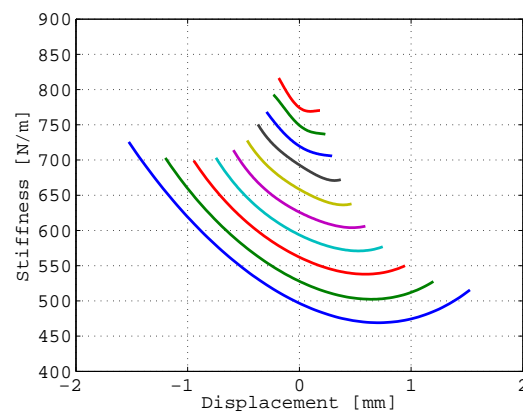


Fig. 7: Mechanical stiffness K_{ms} versus displacement for various excitation levels at 40 Hz.

5. FREQUENCY DEPENDENCE

The previous section has described the new method

of suspension analysis and as an example a 40 Hz harmonic excitation has been chosen for different amplitudes of the excitation signal. In this section, we provide the results for several input frequencies to show the variation of R_{ms} and K_{ms} with frequency.

The loudspeaker is excited at 20, 40, 60 and 80 Hz respectively. The same procedure described above is used for each frequency, and each amplitude of the excitation signal. The same 10 amplitudes of the excitation signal are used according to the previous setup.

In Fig. 8 the resulting mechanical resistance R_{ms} as a function of velocity is plotted. The estimation reveals a decrease of mechanical resistance R_{ms} with frequency. Taking fitted curves at $v = 0$, the mechanical resistance R_{ms} decreases from 1 Ns/m at 20 Hz to 0.4 Ns/m at 80 Hz. Moreover, the mechanical resistance R_{ms} exhibits a positive slope with velocity, the lower the frequency the steeper the slope.

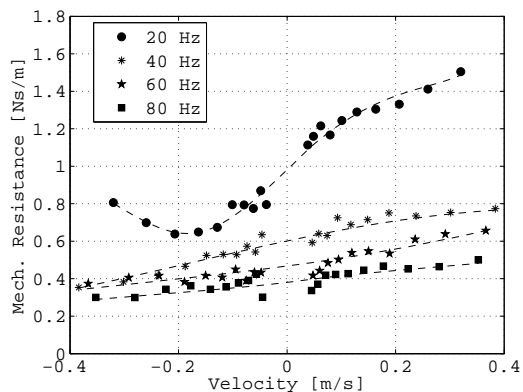


Fig. 8: Mechanical resistance R_{ms} as a function of velocity estimated for frequencies 20, 40, 60 and 80 Hz.

In Fig. 9 the mechanical stiffness K_{ms} is plotted for the same amplitude of excitation signal (2.5 V) and for different frequencies. The excursion gets obviously lower with increasing frequency. The stiffness tends to be lower at low frequencies and slightly increases with higher frequencies.

To compare the stiffness K_{ms} as a function of frequency from the mechanical point of view, differ-

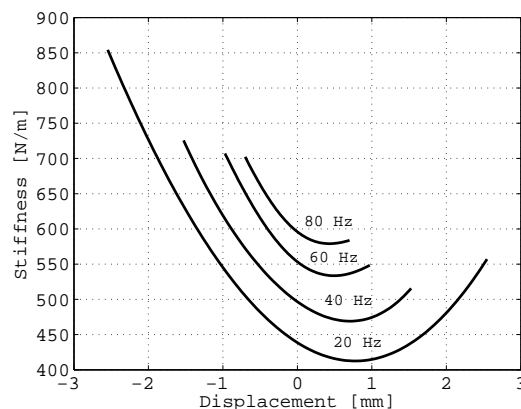


Fig. 9: Mechanical stiffness K_{ms} as a function of displacement estimated for frequencies 20, 40, 60 and 80 Hz when excited with the same input level $U_1 = 2.5$ V.

ent excitation levels are chosen resulting in the same peak displacement. In Fig. 10 the mechanical stiffness K_{ms} is plotted versus displacement for different frequencies, keeping the peak displacement the same (0.7 mm). This comparison shows almost the same curves of K_{ms} as a function of displacement, independently on the frequency.

6. DISCUSSION

The mechanical properties of loudspeakers suspensions are among the most difficult to identify. Suspensions are usually made from impregnated materials whose properties are affected by many physical phenomena. The results presented above show that these phenomena are far from being linear.

The mechanical resistance R_{ms} depicted in Fig. 5 reveals a significant dependency on instantaneous velocity. Fig. 8 shows that the mechanical resistance R_{ms} varies with frequency as well. Not only the slope of the velocity changes (decreases with frequency) but also the value of R_{ms} itself decreases with frequency. The decrease of R_{ms} with frequency has been observed also by Thorborg et al. in [6].

The stiffness K_{ms} depicted in Fig. 7 depends not only on instantaneous displacement as usually considered in nonlinear loudspeaker modeling [8] but also on excitation level or in other words on peak

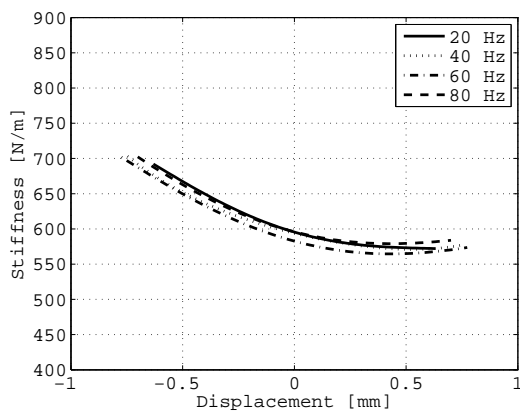


Fig. 10: Mechanical stiffness K_{ms} as a function of displacement estimated for frequencies 20, 40, 60 and 80 Hz. Peak displacement is kept almost the same.

displacement. The necessity to incorporate the peak displacement dependency of the stiffness K_{ms} has already been pointed out by Klippel in [7]. The variation of K_{ms} with frequency is depicted in Figs. 9 and 10 from two different points of view. In Fig. 9, the K_{ms} is plotted for the same excitation levels (2.5 V) resulting in a slight dependency of K_{ms} with frequency. K_{ms} tends to slightly increase with frequency. Thorborg et al. observed in [6] similar symptom in a small amplitude excitation. Keeping the voltage constant corresponds to a standard usage of a loudspeaker since it is most often operated connected to a constant voltage source. Nevertheless, when plotting the K_{ms} as a function of frequency (Fig. 10) and keeping the peak displacement constant (changing appropriately the amplitude of input voltage), the stiffness K_{ms} shows almost no dependency on frequency.

7. CONCLUSION

A new technique for measuring the mechanical stiffness K_{ms} and the mechanical resistance R_{ms} of a loudspeakers suspension has been presented. The technique is based on the assumption of purely harmonic displacement and velocity of the diaphragm. To achieve such a condition an active harmonic control technique to suppress higher harmonics from the displacement signal is used.

The results presented on an arbitrary chosen loudspeaker have shown a dependency of the mechanical stiffness K_{ms} on instantaneous and peak displacement and a dependency of the mechanical resistance R_{ms} on velocity. Moreover, a frequency dependency of these parameters has been discussed.

8. REFERENCES

- [1] N. Thiele, "Loudspeakers in vented boxes: Part 1," *J. Audio Eng. Soc.*, vol. 19, no. 5, pp. 382–392, 1971.
- [2] R. H. Small, "Vented-box loudspeaker systems—part 1: Small-signal analysis," *J. Audio Eng. Soc.*, vol. 21, no. 5, pp. 363–372, 1973.
- [3] M. Rousseau and J. Vanderkooy, "Visco-elastic aspects of loudspeaker drivers," in *118th Audio Engineering Society Convention*, Barcelona, Spain, May 2005.
- [4] M. H. Knudsen and J. G. Jensen, "Low-frequency loudspeaker models that include suspension creep," *J. Audio Eng. Soc.*, vol. 41, no. 1/2, pp. 3–18, 1993.
- [5] K. Thorborg, C. Tinggaard, F. Agerkvist, and C. Futtrup, "Frequency dependence of damping and compliance in loudspeaker suspensions," *J. Audio Eng. Soc.*, vol. 58, no. 6, pp. 472–486, 2010.
- [6] K. Thorborg and C. Futtrup, "Frequency dependence of the loudspeaker suspension (a follow up)," *J. Audio Eng. Soc.*, vol. 61, no. 10, pp. 778–786, 2013.
- [7] W. Klippel, "Dynamic measurement of loudspeaker suspension parts," *J. Audio Eng. Soc.*, vol. 55, no. 6, pp. 443–459, 2007.
- [8] W. Klippel, "Nonlinear large-signal behavior of electrodynamic loudspeakers at low frequencies," *J. Audio Eng. Soc.*, vol. 40, no. 6, pp. 483–496, 1992.